Collaborative Communication in Multi-robot Surveillance Based on Indoor Radio Mapping

Yunlong Wu, Bo Zhang(✉), Xiaodong Yi, and Yuhua Tang

State Key Laboratory of High Performance Computing, College of Computer, National University of Defense Technology, Changsha, China
zhangbo10@nudt.edu.cn

Abstract. This paper considers a scenario where multiple sensing robots are deployed to monitor the indoor environments, and transmit the monitored data to the base station. In order to ensure favorable surveillance quality, we aim at achieving a high throughput for the multi-robot system. We firstly establish the stochastic wireless channel model and derive the expression of the throughput. Then, we propose the non-collaborative and collaborative communication strategies, both adopting the joint frequency-rate adaptation based on the stochastic channel model. The experimental results have shown that the throughput can be largely improved with the collaboration between robots. Furthermore, considering our surveillance scenario is approximate time-invariant (ATI), we propose the joint frequency-rate communication strategies based on proactive channel measurements, and the effectiveness of the strategies is validated by experimental results.

Keywords: Multi-robot collaboration · Joint frequency-rate communication strategies · Relays · Wireless channel modeling

1 Introduction

A multi-robot system aims at achieving challenging tasks or significantly improving mission performance compared with a single robot, which demands consensus and cooperation among robots [1]. In this paper, we consider a scenario where a team of sensing robots are deployed to monitor an indoor area, and transmit the monitored data (e.g., videos) to a base station through wireless communications. In the base station, the data will be analyzed for identifying abnormalities (e.g., an intruder) in the area.

For this multi-robot surveillance scenario, communication planning is demanded for maintaining reliable and high-throughput communications between each sensing robot and the base station. In [2], a rate-configurable robot was deployed to collect the generated data from several points of interest (POIs). A multi-robot communication planning strategy was considered in [3], where the authors aimed at maximizing the connectivity probabilities of the multi-robot

© ICST Institute for Computer Sciences, Social Informatics and Telecommunications Engineering 2017
S. Wang and A. Zhou (Eds.): CollaborateCom 2016, LNICST 201, pp. 211–220, 2017.
DOI: 10.1007/978-3-319-59288-6_19

network by optimizing the routing variables. However, the communication strategies above just consider the case that the robots adopt the fixed communication frequency-allocation.

Against this background, in this paper we propose the joint frequency-rate communication planning and a series of strategies for multi-robot systems. The contributions of this paper are as follows:

In Sect. 2, in order to support the joint frequency-rate communication planning, we firstly establish the multi-frequency wireless channel model which reflects the received signal quality (RSQ) of each communication frequency at each spatial location. Then, the channel model is used to evaluate the communication performance metric (e.g., throughput) and the packet error rate (PER). The distribution of RSQ may be depicted as a stochastic model with three main parts: path loss, shadowing and multipath fading [4]. The multi-robot system can select the optimal frequency-rate setting to maximize the throughput according to the RSQ-location mappings.

In Sect. 3, we propose two joint frequency-rate communication strategies based on the stochastic channel model. The *non-collaborative communication* strategy considers that each sensing robot communicates with the base station, and there is no information exchange among the sensing robots. The *collaborative communication* strategy allows the sensing robots to assist each other by relaying. For example, if a sensing robot is experiencing deep fading, relaying by other robots may greatly improve the throughput for supporting the monitored data transmission [5,6].

In Sect. 4, we pinpoint the fact that the stochastic channel model may capture the distribution of RSQ, however cannot exploit the exact RSQ at different locations for improving the throughput. Therefore, we propose to construct the RSQ-location mapping with proactive channel measurements, which may capture the RSQ more precisely than the stochastic model. Especially, when the RSQ changes rapidly in spatial domain variation, while changing slowly over the time domain. The experimental results have proved that the actual indoor measurements can identify the approximate time-invariant (ATI) scenarios and a higher throughput may be achieved in comparison with the stochastic model-based strategies.

In Sect. 5, the experimental results prove the effectiveness of joint frequency-rate communication planning, the collaboration strategy as well as the proactive channel measurements in improving the throughput of multi-robot systems.

2 Problem Formulation

We assume a N-sensing-robot system is deployed to monitor an area, where the surveillance route of each sensing robot is predefined and periodic. That is to say, when the sensing robot returns to the initial location, it may continue another loop. The sensors equipped on robots are responsible for collecting the environment information, and we may require the monitored data should be transmitted to the base station in real-time. Considering the high data sampling

rates of the sensors on the robots (e.g., 4 Mbps per channel for a 1080P camera), we need to reasonably configure the communication settings, in the context of this paper, the frequency or the modulation and coding patterns, for the sake of maximizing the throughput of the multi-robot network based on the channel quality of the current location.

In order to avoid the interference between sensing robots, we adopt the frequency division multiple access (FDMA) mechanism, where the sensing robots are allocated orthogonal frequency channels for communications. However, we also allow dynamic frequency re-allocation during the operations. In an indoor environment, the geometric structure is often complicated which leads to the high complexity of the wireless communication channel. In order to get an optimal communication setting, we need to predict the received signal power at each spatial location and of multiple frequency bands.

2.1 Wireless Channel Modeling

The wireless communication channel can be modeled as a system affected by path loss, shadowing and multipath fading [7]. Let $G(q, f)$ denote the channel gain for the receiver node at location $q \in \mathcal{W}$ in frequency $f \in \mathcal{F}$, where $\mathcal{W} \subset \mathbb{R}^2$ is the workspace and $\mathcal{F}$ is the set of all candidate frequencies. Therefore, $G(q, f)$ can be expressed as $G(q, f) = G_{\mathrm{PL}}(q, f) G_{\mathrm{SH}}(f) G_{\mathrm{MP}}$, where $G_{\mathrm{PL}}(q, f)$ is the distance-dependent path loss. $G_{\mathrm{SH}}(f)$ and G_{MP} represent the impacts of shadowing and multipath fading respectively. G_{MP} can be regarded as a random variable having a mean value of 1. Let $P_{\mathrm{RX}}(q, f)$ denote the received signal power at $q \in \mathcal{W}$ in frequency $f \in \mathcal{F}$. We have $P_{\mathrm{RX}}(q, f) = P_{\mathrm{TX}} G(q, f)$, where P_{TX} is the transmit power from a fixed transmitter at $q_{\mathrm{TX}} \in \mathcal{W}$ and can be treated as a constant. Let $P_{\mathrm{RX,dB}}(q, f) = 10\log_{10}(P_{\mathrm{RX}}(q, f))$ represent the received signal power in dB. We have

$$\begin{aligned} P_{\mathrm{RX,dB}}(q, f) = & K_{\mathrm{PL,dB}}(f) + 10 n_{\mathrm{PL}}(f) \log_{10} \|q - q_{\mathrm{TX}}\| \\ & + K_{\mathrm{SH,dB}}(f) + \omega_{\mathrm{MP,dB}}. \end{aligned} \tag{1}$$

In Eq. (1), $K_{\mathrm{PL,dB}}(f)$ and $n_{\mathrm{PL}}(f)$ are the path loss parameters respectively. $\|q - q_{\mathrm{TX}}\|$ represents the distance between the transmitter and the receiver at $q \in \mathcal{W}$. $K_{\mathrm{SH,dB}}(f)$ is set according to if there existing shadowing. When there is no line-of-sight (LOS) communication channel, $K_{\mathrm{SH,dB}}(f)$ is non-zero. If a LOS channel exists, $K_{\mathrm{SH,dB}}(f) = 0$. $\omega_{\mathrm{MP,dB}}$ is a zero-mean random variable which represents the multipath fading effect in dB.

2.2 Parameters Estimation

The parameters of Eq. (1) contains $K_{\mathrm{PL,dB}}(f)$, $n_{\mathrm{PL}}(f)$, $K_{\mathrm{SH,dB}}(f)$ and $\omega_{\mathrm{MP,dB}}$. In order to estimate the parameters, we designed a radio-mapping robot by mounting a universal soft-defined radio peripheral (USRP) device on a TurtleBot robot. We scheduled the robot to move along a trajectory in the LOS and non-ling-of-sight (NLOS) areas respectively, while recording the signal power along

the route. Figure 1a and b, for instance, show the received power in dB along a LOS route and a NLOS route in our laboratory with three frequencies: 900 Hz, 1.8 GHz and 2.6 GHz. We may fit the measured data with a linear function based on least-square estimation. The fitting parameters are shown in Fig. 1a and b, where n_{PL} denotes the slope of the linear functions. In the LOS case, the intercept is $K_{\mathrm{PL,dB}}(f)$. While, in the NLOS case, the intercept is $K_{\mathrm{PL,dB}}(f) + K_{\mathrm{SH,dB}}(f)$. It is shown that the path loss parameters of different frequencies are also different. As the frequency increases, the path loss parameters are more significant. In the LOS or NLOS area, the parameters are also different.

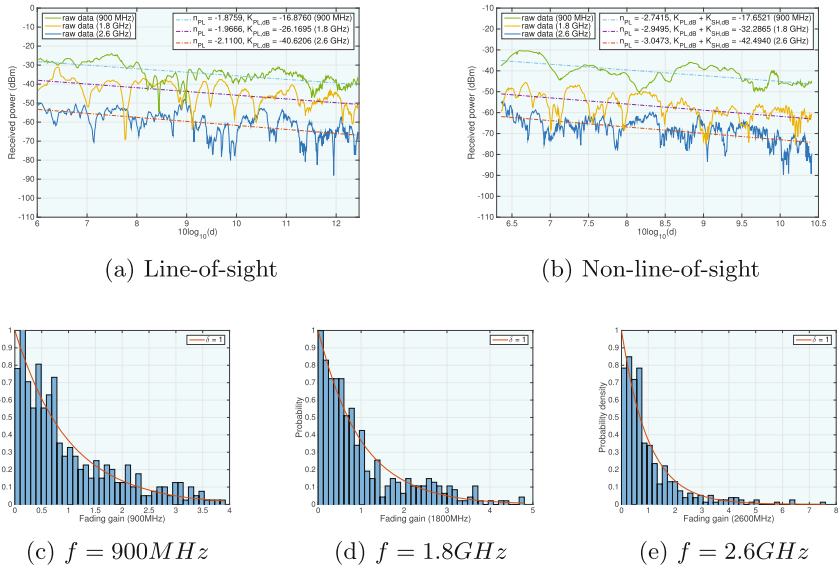

(a) Line-of-sight (b) Non-line-of-sight

(c) $f = 900MHz$ (d) $f = 1.8GHz$ (e) $f = 2.6GHz$

Fig. 1. Line-of-sight (a) and non-line-of-sight (b) path loss parameter estimation in 900 MHz, 1.8 GHz and 2.6 GHz. Rayleigh distribution fitting in 900 MHz (c), 1.8 GHz (d) and 2.6 GHz (e).

The distribution of the fading effect is often based on specific environments. In the literatures, the variable ω_{MP} ($\omega_{\mathrm{MP}} = 10^{\omega_{\mathrm{MP,dB}}/10}$) follows some classical distribution models, such as Nakagami, Rayleigh or Rician [8]. For estimating the random variable ω_{MP}, we may extract samples in a NLOS area and ensure the distance from the sampling location to the base station does not change significantly and there is constant shadowing. In Fig. 1c to e, for instance, we collect about 500 samples for 900 MHz, 1.8 GHz and 2.6 GHz respectively, and draw the normalized histogram for each case. The results show that the ideal Rayleigh distribution (the line with $\delta = 1$) may fit the measurements well. Therefore, in this paper, we assume ω_{MP} follows the ideal Rayleigh distribution.

2.3 Rate Adaptation

Transmission rates may be adapted by selecting different combinations of channel coding and modulations. In this subsection, we may use the received signal-to-noise ratio (SNR) to derive the expression of the optimal transmission rate. We adopt the adaptive modulation and coding (AMC) scheme in 802.11n protocols, where SNR-triggered rate-selection allows adaptively choosing from a set of 6 transmission rates [9]. According to [9], the per-hop PER model is given by: $\mathrm{PER}_n(\gamma) = a_n \exp(-g_n\gamma)$ if $\gamma \geq \gamma_{pn}$ and $\mathrm{PER}_n(\gamma) = 1$ if $0 < \gamma < \gamma_{pn}$, where γ is the instantaneous received SNR, γ_{pn} is the switch threshold, and a_n, g_n are relative to the transmission mode index n, which represents the specific modulation and transmission rate as shown in Table II of [9]. We assume the wireless fading channel is quasi-static and Rayleigh distributed [7], then the resulted per-hop PER is

$$\begin{aligned}\mathrm{PER}_n(\overline{\gamma}) &= \int_0^{+\infty} \mathrm{PER}_n(\gamma)\frac{1}{\overline{\gamma}}\exp\left(-\frac{\gamma}{\overline{\gamma}}\right)d\gamma \\ &= 1-\exp\left(-\frac{\gamma_{pn}}{\overline{\gamma}}\right)+\frac{a_n}{\overline{\gamma}g_n+1}\exp(-g_n\gamma_{pn})\exp\left(-\frac{\gamma_{pn}}{\overline{\gamma}}\right),\end{aligned} \tag{2}$$

where $\overline{\gamma}$ is the average received SNR. In order to guarantee the communication quality, the PER of each sensing robot to the base station should be below a predefined threshold p_{ub}. In other words, when given p_{ub}, we may obtain the SNR thresholds for each mode. However, deriving the inverse function of Eq. (2) directly may be difficult. As an alternative, we may calculate $\mathrm{PER}_n(\overline{\gamma})$ by enumerating all possible values of $\overline{\gamma}$ for each mode. When given p_{ub}, we may look up the most similar SNR threshold $\overline{\gamma}_{n,\mathrm{ub}}$ for each mode n. Therefore, according to the average received SNR $\overline{\gamma}$, we may derive the optimal transmission mode n^* and transmission rate R^* as: $n^* = \arg\min_n\left(\overline{\gamma}-\overline{\gamma}_{n,\mathrm{ub}}\right), \forall\ \overline{\gamma}_{n,\mathrm{ub}} \leq \overline{\gamma}$, $R^*{=}R(n^*)$.

2.4 Throughput Modeling

The metric of throughput is often used to measure the data transmission capability of a communication network. For the sake of numerical analysis, we discretize the surveillance route (with length of L) into M steps, and the length of each step is $\Delta l = L/M$. We assume every sensing robot surveys the indoor environment with the constant speed v. Therefore, the time consumption by the sensing robot moving a distance of Δl is $\Delta t = \Delta l/v$. In surveillance applications, each sensing robot should achieve a favorable throughput. Therefore, the throughput $\mathcal{T}$ of the system can be modeled as a minimum-rate expression

$$\mathcal{T} = \frac{\sum_{i=1}^{M}\left(\min\left(R_1^i, R_2^i, ..., R_N^i\right)\Delta t\right)}{M\Delta t}, \tag{3}$$

where R_j^i represents the transmission rate of the j-th sensing robot in the i-th step. In each step, R_j^i is assumed fixed. Equation (3) shows that the communication performance of the system is dominated by the sensing robot with the minimum transmission rate.

3 Joint Frequency-Rate Communication Based on Stochastic Fading Modeling

3.1 Non-collaborative Communication Strategy

According to the analysis and experimental results, we may adjust the per-robot throughput by jointing frequency allocation and rate adaptation. According to Eq. (1), we may derive the average received power at each spatial location $q \in \mathcal{W}$ and frequency $f \in \mathcal{F}$. Figure 2a to c, for instance, show the distribution of the average received power in a rectangle indoor area for three different frequencies, where the base station is located in the southwest corner. Due to the effects of shadowing and path loss, the average received signal quality in the northeast corner of the map may be the worst. Given the same transmit power, the average received power of a lower frequency may be higher than that of a higher frequency. Therefore, we may propose a strategy that, in the worse channel-quality area based on the prediction results, a reliable frequency and modulation pattern may be adopted. We also assume the average noise power at each robot is identical. Let $\overline{\gamma}_i$ denote the predicted average SNR of the i-th robot, and further assume $\overline{\gamma}_1 > \overline{\gamma}_2 > \cdots > \overline{\gamma}_N$. We have the frequency allocation as $f_1 > f_2 > \cdots > f_N$, where f_i is the communication frequency of the i-th robot. When the frequency allocation is finished, each sensing robot can select the optimal transmission rate with the method in Subsect. 2.3.

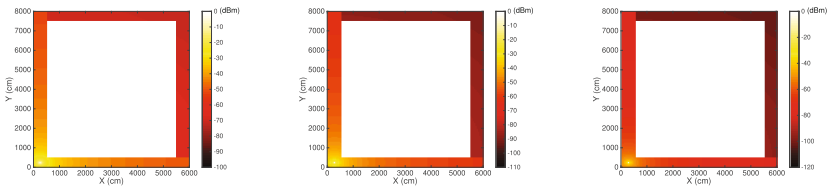

(a) $f = 900MHz$ (b) $f = 1.8GHz$ (c) $f = 2.6GHz$

Fig. 2. Received signal power prediction for different frequencies.

3.2 Collaborative Communication Strategy

The non-collaborative strategy does not exploit the inter-robot channels, which may provide additional degree-of-freedom for improving the throughput. Therefore, we propose the collaborative communication strategy, where a sensing robot can also provide communication relaying for other sensing robots. However, as

the half-duplex wireless device is considered, the robot acting as a relay may sacrifice its own transmission resources for the sake of assisting other robots. Against this interesting trade-off, we will formulate the optimization problem of the collaborative strategy and evaluate its throughput performance. Let R_i denote the allowed transmission rate of the i-th node ($i = 0$ represents the base station and $i \neq 0$ represents the sensing robot), which can be expressed as the difference between the outgoing and incoming rates

$$R_i\left(\boldsymbol{F}, \boldsymbol{\lambda}\right) = \begin{cases} \underbrace{\sum_{j=0, j\neq i}^{N} \lambda_{i,j} R_{i,j}}_{\text{outgoing}} - \underbrace{\sum_{j=1, j\neq i}^{N} \lambda_{j,i} R_{j,i}}_{\text{incoming}}, \forall i \neq 0, \\ \infty - \sum_{j=1, j\neq i}^{N} \lambda_{j,i} R_{j,i}, i = 0, \end{cases} \tag{4}$$

where $\lambda_{i,j}$ is the fraction of time from the i-th node to the j-th node, and $R_{i,j}$ is the corresponding transmission rate. We further define vectors $\boldsymbol{F} = (f_1, f_2, ..., f_N), f_i \in \mathcal{F}$, $\boldsymbol{R} = (R_{1,0}, ..., R_{N,N-1}) \in \mathbb{R}^{N^2}$ and $\boldsymbol{\lambda} = (\lambda_{1,0}, ..., \lambda_{N,N-1}) \in \mathbb{R}^{N^2}$. The base station ($i = 0$) is the destination of all information flows. To guarantee that we can find the optimal communication strategy, we set its outgoing rate an infinity. Equation (3) indicates that maximizing the thoughput $\mathcal{T}$ is equivalent to maximizing the minimum transmission rate of the multi-robot system in each step, which can be formulated as an optimization problem shown by Eq. (5).

$$\begin{aligned} \max_{\boldsymbol{F}, \boldsymbol{\lambda}} \quad & \mathcal{J} = \min\left\{R_0\left(\boldsymbol{F}, \boldsymbol{\lambda}\right), R_1\left(\boldsymbol{F}, \boldsymbol{\lambda}\right), ..., R_N\left(\boldsymbol{F}, \boldsymbol{\lambda}\right)\right\} \\ s.\ t. \quad & 1 \geq \lambda_{i,j} \geq 0, \forall i, j, \\ & \sum_{j=1}^{N} \lambda_{i,j} \leq 1, \forall i \neq 0, \\ & R_i\left(\boldsymbol{F}, \boldsymbol{\lambda}\right) \geq 0, \forall i, \\ & f_i \neq f_j, \forall i \neq j, i \neq 0, j \neq 0. \end{aligned} \tag{5}$$

Considering the variable f_i can only be assigned several discrete values, we may separate the variable f_i from the Eq. (5) and get the optimization problem with a specific $\boldsymbol{F}$, as shown in Eq. (6). To find the optimal communication strategy, we may compare the optimized results of Eq. (6) for different frequency settings $\boldsymbol{F}$, and get the optimal one.

$$\begin{aligned} \min_{\boldsymbol{\lambda}} \quad & \mathcal{J}_{\boldsymbol{F}} = \max\left\{-R_0\left(\boldsymbol{\lambda}\right), -R_1\left(\boldsymbol{\lambda}\right), ..., -R_N\left(\boldsymbol{\lambda}\right)\right\} \\ s.\ t. \quad & 1 \geq \lambda_{i,j} \geq 0, \forall i, j, \\ & \sum_{j=1}^{N} \lambda_{i,j} \leq 1, \forall i \neq 0, \\ & R_i\left(\boldsymbol{\lambda}\right) \geq 0, \forall i. \end{aligned} \tag{6}$$

$-R_i\left(\boldsymbol{\lambda}\right)$ is a linear function of $\boldsymbol{\lambda}$, which is also convex. We may set a variable θ that satisfies $0 \leq \theta \leq 1$ and $\boldsymbol{\lambda}_1, \boldsymbol{\lambda}_2 \in \mathbf{dom}\ \mathcal{J}_{\boldsymbol{F}}$, and prove the function $\mathcal{J}_{\boldsymbol{F}}$

is convex by definitions: $\mathcal{J}_{\boldsymbol{F}}\left(\theta\boldsymbol{\lambda}_1+(1-\theta)\,\boldsymbol{\lambda}_2\right) \leq \theta\mathcal{J}_{\boldsymbol{F}}\left(\boldsymbol{\lambda}_1\right)+(1-\theta)\,\mathcal{J}_{\boldsymbol{F}}\left(\boldsymbol{\lambda}_2\right)$. Therefore, Eq. (6) is a convex optimization problem, which can be solved optimally by numerical optimization methods, for example the interior point method.

4 Joint Frequency-Rate Communication Based on Channel Measurements

According to the analysis and experiments in Sect. 2 as well as widely acknowledged in the literature [8], the complex interactions between the environments and the electro-magnetic waves make the exact channel quality of a given location/frequency hard to predict. For example, as shown in Fig. 1a and b, there exists some deep fading locations that cannot be effectively predicted. By assuming the fading effect is a random process, the stochastic model in Sect. 2 aims at finding the fading distribution rather than predicting the actual channel quality of each location/frequency.

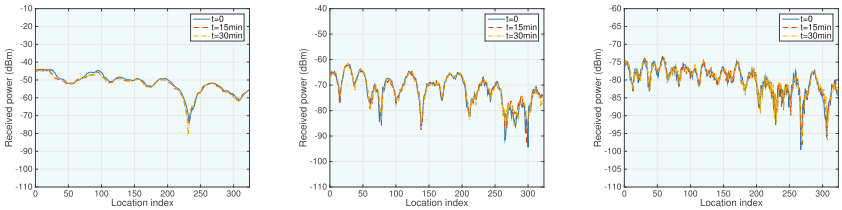

(a) $f = 900MHz$ (b) $f = 1.8GHz$ (c) $f = 2.6GHz$

Fig. 3. Received signal power of different frequencies in the same area every 15 min.

In this paper, we propose another way to circumvent the problem by proactive channel measurements and radio mapping. We may take samples in the whole area densely and construct a realistic RSQ-location mapping based on channel measurements. The mapping can be updated by the sensing robot every few minutes. In a quasi-static environment, such as our indoor scenario, the mapping remains static during a period of time, which is verified by our experimental measurements. Specifically, we measure the received signal power of different frequencies when time $t = 0, 15, 30$ min in the same area, and the results are shown in Fig. 3. The figure demonstrates that the received signal power changes rapidly as the robot moves along a trajectory because of fading. However, the fading pattern changes slowly over time, which allows the measurements of a robot to be effectively utilized by other robots. Therefore, designing communication strategies based on such a measurement-based RSQ-location mapping may benefit a lot than the model-based prediction, as shown in Sect. 5.

5 Experimental Results

In this section, we may compare the effectiveness of different communication strategies. The workspace for experimentation is a 60 m × 80 m rectangle region, and three sensing robots are deployed to survey the corridors of an indoor environment. The surveillance route is divided into 520 discrete segments (steps). In each step, we assume the communication settings may not change. The base station is located at the southwest corner of the workspace. The experiments test all five strategies proposed in this paper, as shown in Table 1. Figure 4a demonstrates the optimized minimum transmission rate of a complete surveillance period of the five communication strategies. With the fixed frequency allocation, the communication of the multi-robot system is interrupted ($\mathcal{J} = 0$) in most of time. When incurring dynamic reconfiguration of frequency and transmission mode, the performance gain is apparent. However, this strategy just considers the data transmission between the sensing robot and the base station, and ignores the collaboration between sensing robots. In the third strategy, we explore the performance gain based on collaborative communications, and the communication interrupts are improved significantly. Moreover, when taking the realistic channel measurements into consideration, the number of communication interrupts is greatly reduced, which is shown in Fig. 4a. The detailed number of interrupts and the throughput for the five strategies are shown in Table 1.

Table 1. Experiment design and results

Strategy index	Description	Interrupts	Throughput
1	Fixed frequency allocation	411	0.1995
2	Model-based non-collaboration	216	0.5995
3	Model-based collaboration	160	0.6995
4	Measurement-based non-collaboration	147	0.7476
5	Measurement-based collaboration	38	1.1459

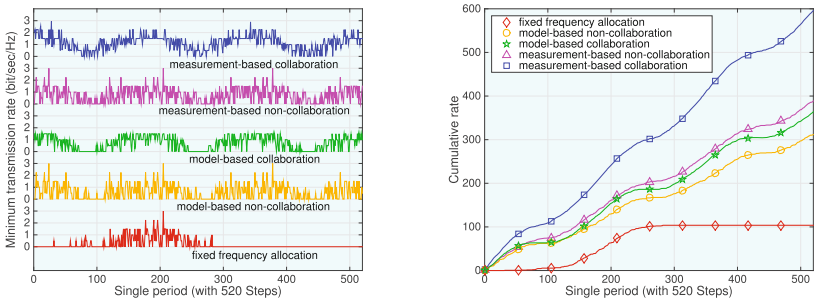

(a) (b)

Fig. 4. Minimum transmission rate (a) and cumulative minimum transmission rate (b) in each step of a complete surveillance period, which contains 520 steps.

We also record the cumulative minimum transmission rate of a complete surveillance period, as shown in Fig. 4b. We may conclude that, compared with the model-based and fixed frequency allocation strategies, the performance gain of the collaborative strategies with realistic channel measurements is evident.

6 Conclusion

In this paper, we considered a multi-robot surveillance scenario and explored the communication performance gain with and without collaboration between robots. In order to achieve this objective, we modeled the wireless channel and throughput of the multi-robot system, and proposed the communication strategies based on the priori channel model and realistic measurements respectively. Furthermore, we proposed the concepts of non-collaborative communication and collaborative communication. The simulations compared the communication performance of different strategies and showed that the measurement-based collaborative communication may obtain a higher throughput and a smaller number of communication interrupts.

References

1. Olfati-Saber, R., Fax, J.A., Murray, R.M.: Consensus and cooperation in networked multi-agent systems. Proc. IEEE **95**(1), 215–233 (2007)
2. Yan, Y., Mostofi, Y.: To go or not to go: on energy-aware and communication-aware robotic operation. IEEE Trans. Control Netw. Syst. **1**(3), 218–231 (2014)
3. Fink, J., Ribeiro, A., Kumar, V.: Robust control for mobility and wireless communication in cyber-physical systems with application to robot teams. Proc. IEEE **100**(1), 164–178 (2012)
4. Yan, Y., Mostofi, Y.: Co-optimization of communication and motion planning of a robotic operation under resource constraints and in fading environments. IEEE Trans. Wirel. Commun. **12**(4), 1562–1572 (2013)
5. Han, B., Li, J., Su, J., Cao, J.: Self-supported cooperative networking for emergency services in multi-hop wireless networks. IEEE J. Sel. Areas Commun. **30**(2), 450–457 (2012)
6. Liang, W., Luo, J., Xu, X.: Network lifetime maximization for time-sensitive data gathering in wireless sensor networks with a mobile sink. Wirel. Commun. Mob. Comput. **13**(14), 1263–1280 (2013)
7. Lindhé, M., Johansson, K.H.: Using robot mobility to exploit multipath fading. IEEE Wirel. Commun. **16**(1), 30–37 (2009)
8. Malmirchegini, M., Mostofi, Y.: On the spatial predictability of communication channels. IEEE Trans. Wirel. Commun. **11**(3), 964–978 (2012)
9. Liu, Q., Zhou, S., Giannakis, G.B.: Cross-layer combining of adaptive modulation and coding with truncated ARQ over wireless links. IEEE Trans. Wirel. Commun. **3**(5), 1746–1755 (2004)